

Supplement of Atmos. Chem. Phys., 18, 6661–6677, 2018
<https://doi.org/10.5194/acp-18-6661-2018-supplement>
© Author(s) 2018. This work is distributed under
the Creative Commons Attribution 3.0 License.



Supplement of

Photochemical aging of aerosol particles in different air masses arriving at Baengnyeong Island, Korea

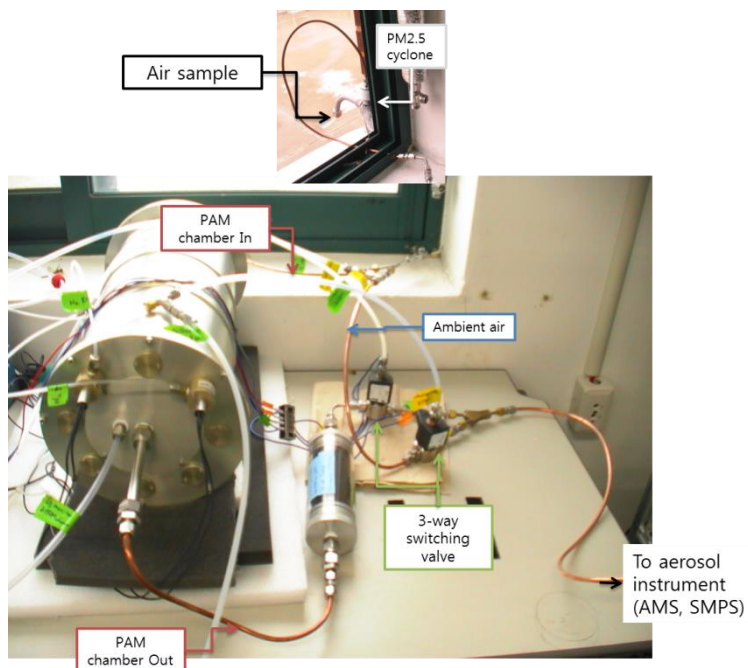
Eunha Kang et al.

Correspondence to: Meehye Lee (meehye@korea.ac.kr)

The copyright of individual parts of the supplement might differ from the CC BY 3.0 License.

1 S1. The sampling setup of the PAM reactor

2
3
4
5



6
7
8

[Figure S1. The PAM reactor sampling setup]

9 In our experimental setup, the PAM reactor was installed beside the window in the
10 laboratory and ambient air was pulled through a copper tubing (~ 30 cm)
11 cyclone outside the laboratory. The ambient air from the PM2.5 cyclone was introduced
12 into the PAM reactor through an inlet plate and endcap and then rapidly dispersed
13 before entering the reactor through a Silconert-coated (Silcotech, Inc.) stainless steel
14 screen. Aerosol sampling tubes were 1/4 inch OD copper and stainless steel tubes and
15 gas sampling tubes were 1/4 inch OD PTFE Teflon tubes. The ambient and PAM reactor
16 through air samples were alternately switched to the aerosol measurement instruments
17 by using a 3-way switching valve every 6 minute. The 3-way switching valve might cause
18 the evaporation of ambient and PAM aerosols when it was getting hot during operation.
19 When PAM aerosol was introduced in the measurement instruments, ambient aerosol was
20 bypassed to outside and vice versa. The total flow rate to the PAM reactor and ambient

21 sampling was set to 5 liters per minute. We tried to set up the PAM reactor as close as
22 possible to the PM2.5 cyclone and the AMS/SMPS instruments as shown in the figure
23 above. The aerosol particles and gases loss due to the PAM reactor and through the tube
24 surfaces contributes to the mass concentration measurement uncertainty.

25

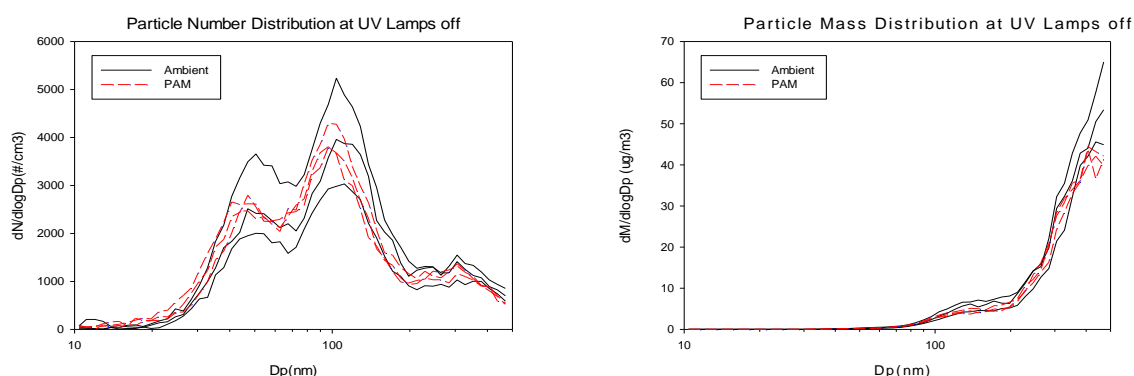
26 S2. The wall loss test

27 We conducted the loss test for 1) ambient aerosol and 2) SO₂ during the experiment in
28 2011. Its results are discussed below and the LVOCs fate is calculated using the method
29 in Palm et al. (2016).

30

31 First, PAM reactor was run for ambient air without lamp-on and the SMPS signals of air
32 entering and exiting the PAM reactor were compared to estimate the physical loss of
33 aerosol to the wall. In experimental setup, ambient air entering the PAM reactor was
34 introduced into SMPS alternately with air exiting the PAM reactor. For the test, this cycle
35 was repeated three times. Because entering and exiting air was not simultaneously
36 measured, there could be some error caused by the variation of ambient air. However,
37 there was no detectable variation in ambient air, judged from gaseous concentrations for
38 less than an hour of test period. The mass of ambient aerosol and aerosol exiting the
39 PAM reactor (without lamps on) was $13.1 \pm 2.06 \mu\text{g m}^{-3}$ and $11.6 \pm 0.46 \mu\text{g m}^{-3}$,
40 respectively, resulting in about 12 % of aerosol mass in the PAM reactor (Figure below).
41 However, the decrease in mass was due to the loss of pre-existing aerosols but not newly
42 formed secondary aerosols from condensable gases.

43

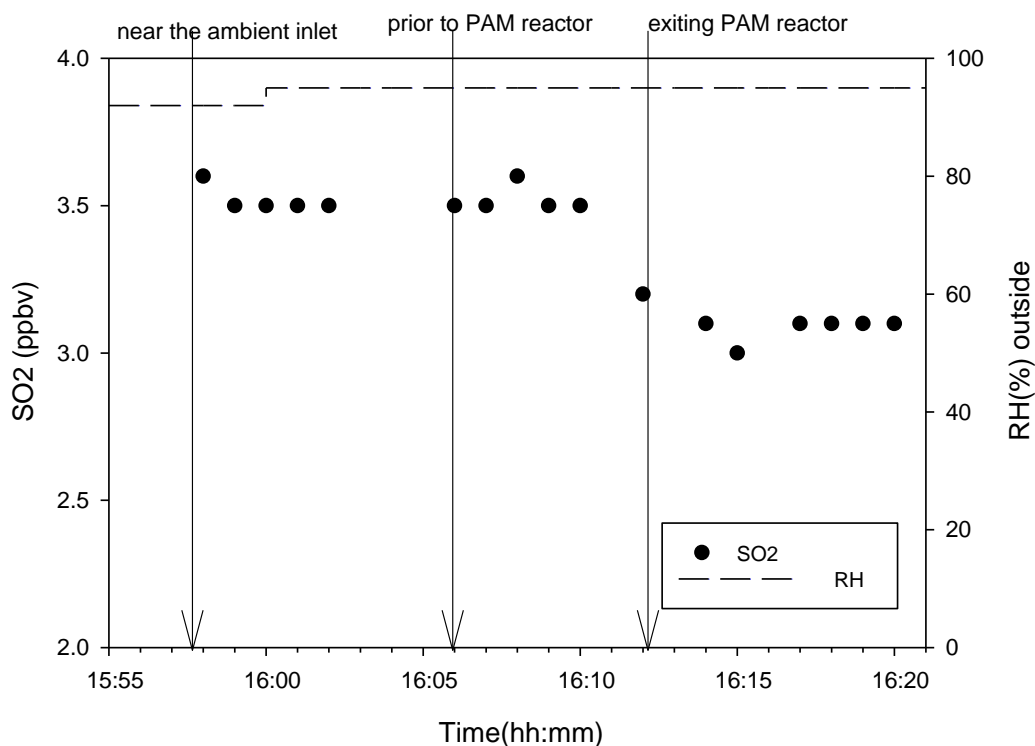


44

45 [Figure S2-1. SMPS particle number distribution (left) and mass distribution (right) for wall
46 loss test. Red and black color indicate air exiting and entering the PAM reactor.]

47

48 Second, we have tested SO₂ loss by the wall during the experiment. For this test, we used
49 ambient air instead of standard SO₂ mixtures in a wide range of concentrations. When air
50 was pulled through the PAM reactor inlet plate, SO₂ was measured first for ambient air in
51 front of the inlet, and then before it entered and after it exited the PAM reactor (Figure
52 below). SO₂ concentrations prior to and after the PAM reactor were 3.5 ppbv and 3.1
53 ppbv, respectively, leading to SO₂ loss of 11 ± 7 %. There was loss in the sampling inlet
54 line. The detailed information on SO₂ measurement is given below.



55

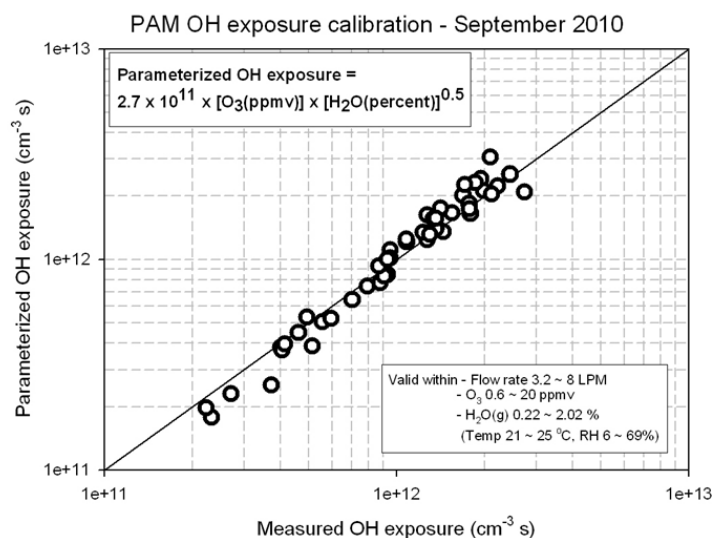
56

[Figure S2-2. SO₂ loss test results in PAM reactor]

57

58 S3. Calibration of OH exposure in the PAM reactor

59 We used the OH exposure calibration which was done with a mixture of pure air and
60 SO₂(g) in the laboratory by Kang et al. (2011a). The full manuscript can be found in J.
61 KOSAE Vol. 27, No. 5 (2011) pp. 534~544, Journal of Korean Society for Atmospheric
62 Environment, DOI: <http://dx.doi.org/10.5572/KOSAE.2011.27.5.534>.



63
 64 [Figure S3. OH exposure calibration curve for this PAM reactor. (cited from Kang et al.,
 65 (2011a)]
 66

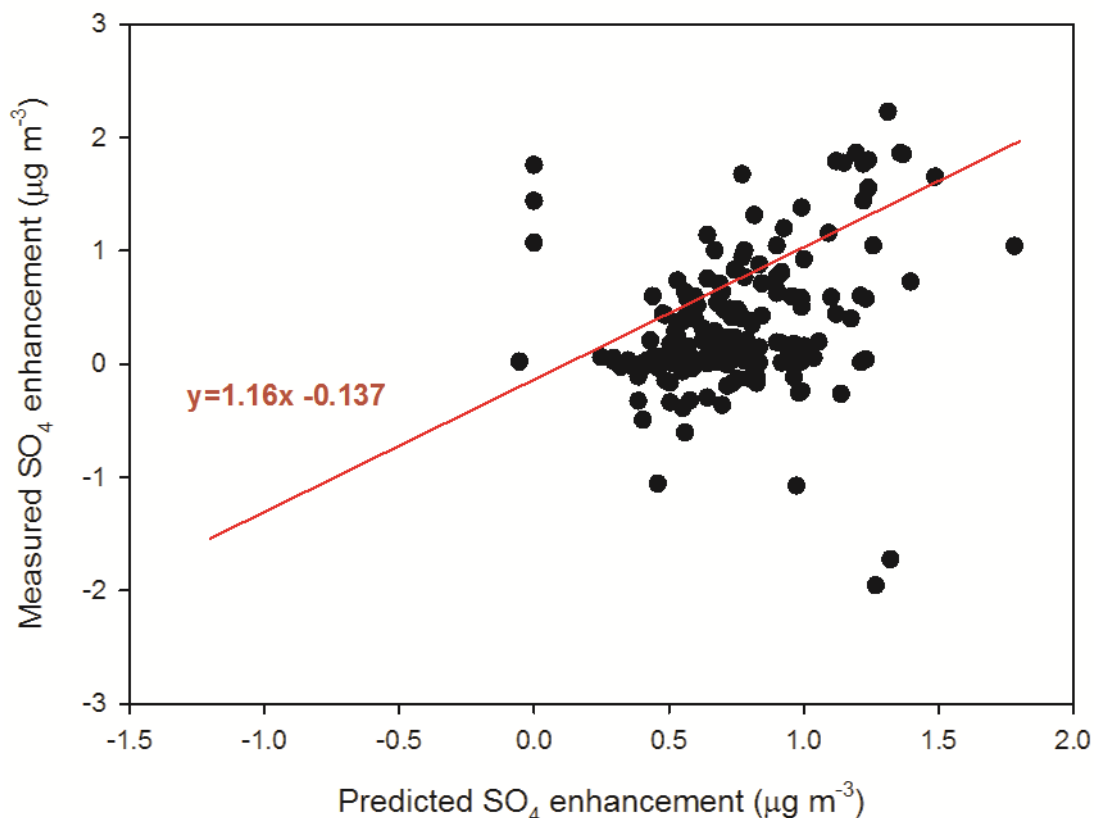
67 S4. Comparison between calculated and measured sulfate formation in PAM reactor

68 We calculated the sulfate formation using SO₂ measurements from sampling through and
 69 bypassing the PAM chamber, assuming that SO₂(g) was converted to sulfate(p) by
 70 reaction with OH inside the PAM reactor. For this estimation, we adopted 2 ppbv offset
 71 for ambient SO₂ measurement, SO₂ gas loss of 11 % in the PAM reactor, and condensable
 72 sulfate loss by wall and exiting the reactor of about 38%. At 4.6 days of OH exposure, 43%
 73 of SO₂ will be consumed in the PAM reactor based on $k_{\text{SO}_2+\text{OH}} = 1 \times 10^{-12} \text{ cm}^3 \text{ molec}^{-1} \text{ s}^{-1}$.
 74 The measured SO₄ enhancement was obtained by subtracting the ambient SO₄
 75 concentration from the SO₄ concentration measured in PAM chamber. For this
 76 comparison, AMS measurements were averaged hourly to be consistent with the SO₂
 77 measurement. The figure below compares the measured and predicted SO₄ enhancement,
 78 showing that the measured explained well the expected (slope = 1.16 and an intercept =
 79 -0.137. We used the total least squares regressions ([http://www.real-
 80 statistics.com/regression/total-least-squares/](http://www.real-statistics.com/regression/total-least-squares/)), which is minimizing the sum of the squared
 81 Euclidean distances from the points to the regression line similar to orthogonal distance
 82 regression. The correlation between the measured and predicted was deteriorated by the
 83 very low measured SO₄ enhancement against a wide range of sulfate expected to be
 84 enhanced. Not to mention, uncertainty was involved in the measurement of SO₂

85 concentration, loss assessment of SO₂ and condensable sulfate, and the AMS
86 measurement of particles smaller than 50 nm.

87

88



89

90 [Figure S4. Measured SO₄ enhancement vs. calculated SO₄ enhancement.]

91

92

93 S5. Estimating the condensation sink

94 In addition, we estimated the loss of condensable gases by wall deposition, exiting the
95 reactor, and further OH reaction competing with condensation on existing particles,
96 based on Palm et al. (2016) and model posted in <https://sites.google.com/site/pamwiki/hardware/estimation-equations>. Although the model calculating the possible loss of
97 condensable gases was developed a couple of years after this experiment was performed,
98 the physical setup of our PAM reactor was very similar to the ones used in Palm et al.
99 (2016), Ortega et al. (2013), and (2016).

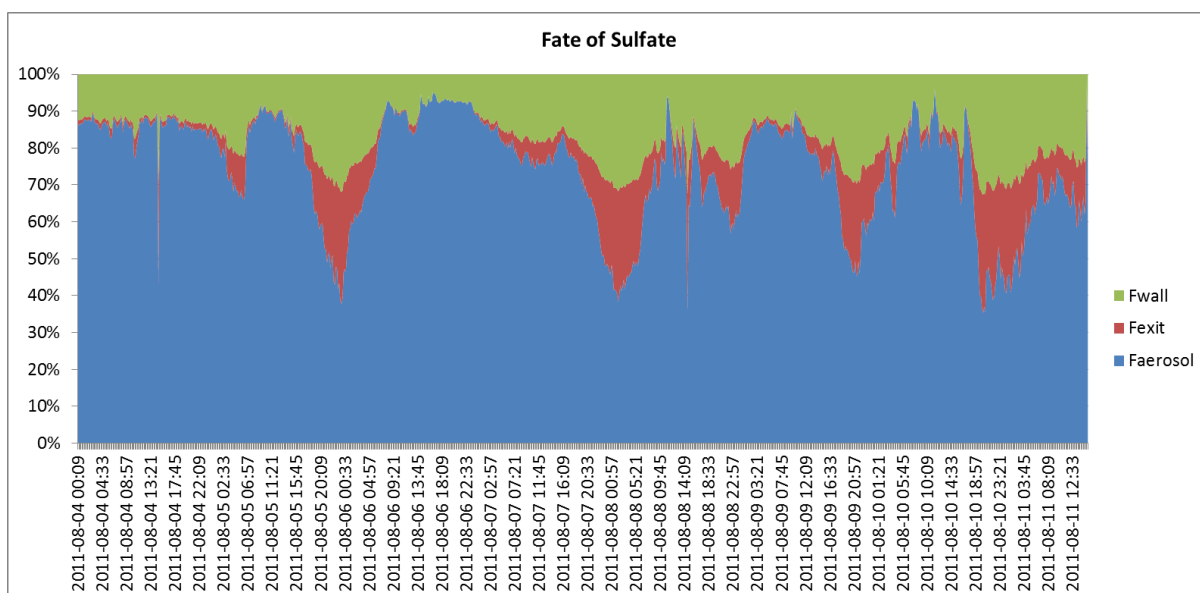
100

102 We used the same constants as those in Palm et al. (2016), but for wall loss in our
103 experiment, we used a measured loss percentage of SO₂ of 11%. A proportion to
104 condensing on the existing particles (Faerosol denoted in Figure S5) associates to the
105 condensation sink (CS). The details of aerosol CS calculation were available in a previous
106 paper (Salimi et al., 2015). Faerosol variation with respect to time was due to the existing
107 particles concentration variation. About 20~70% of condensable organic gases were
108 estimated to be condensed on existing particles, contributing to mass increase in PAM
109 reactor. It is similar to the case of high condensation sink (CS) shown in figure 5 of Palm
110 et al. (2016). In our study the fraction of low-volatility gases that were not condensed in
111 the PAM reactor was higher for organic-dominated case (~40%) than sulfate-dominated
112 case (~30%) because of greater CS in latter than former.

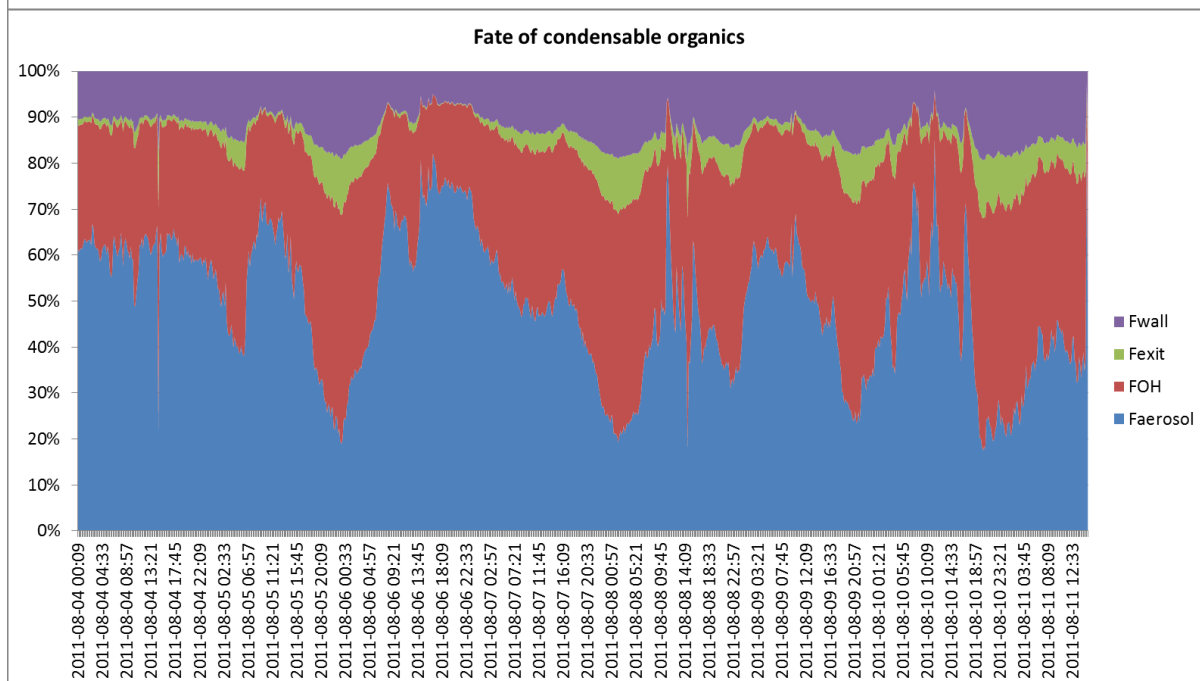
113
114 For conversion of SO₂ to sulfate, the fraction of additional OH reaction-induced loss was
115 set to 0 because of no more reactions between SO₂ and OH as described in Palm et al.
116 (2016). The estimated fraction of sulfate condensation on existing particles was in the
117 range of 40~90% and the rest were expected to be lost by walls and exit the reactor
118 without being condensed.

119
120
121
122
123
124
125
126
127
128
129
130
131
132
133
134
135

136



137



138

139 [Figure S5. Fractional loss of SO₂ (upper) and condensable organics (down) in PAM
140 reactor]

141

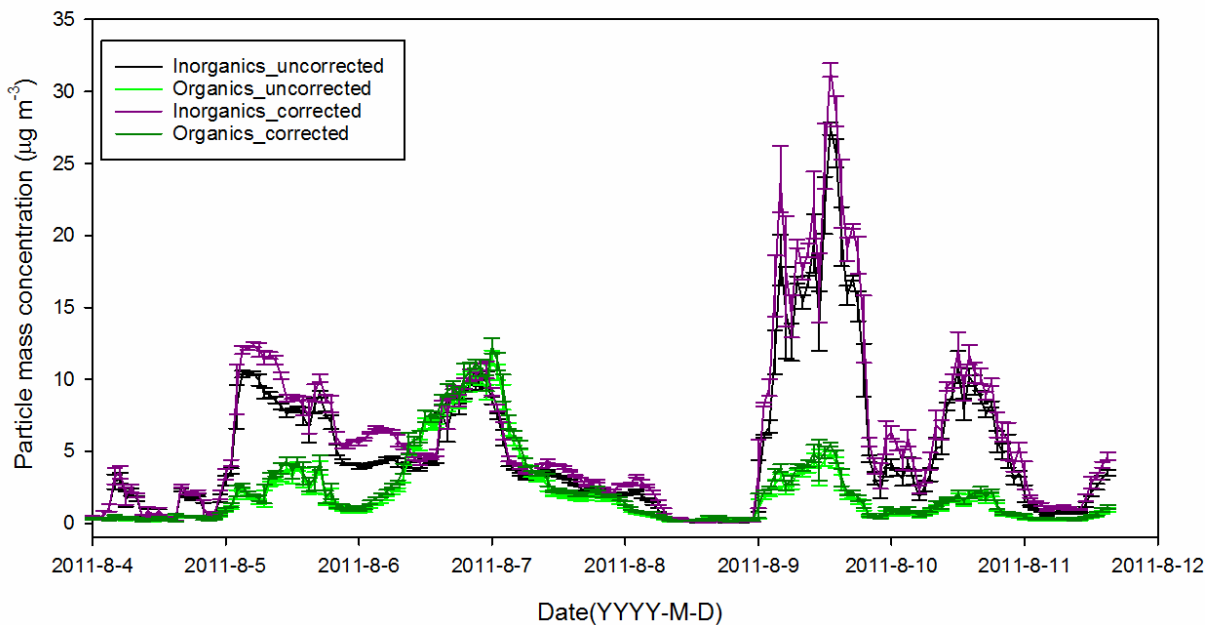
142

S6. Correction of the particle mass concentration in PAM reactor with condensation loss

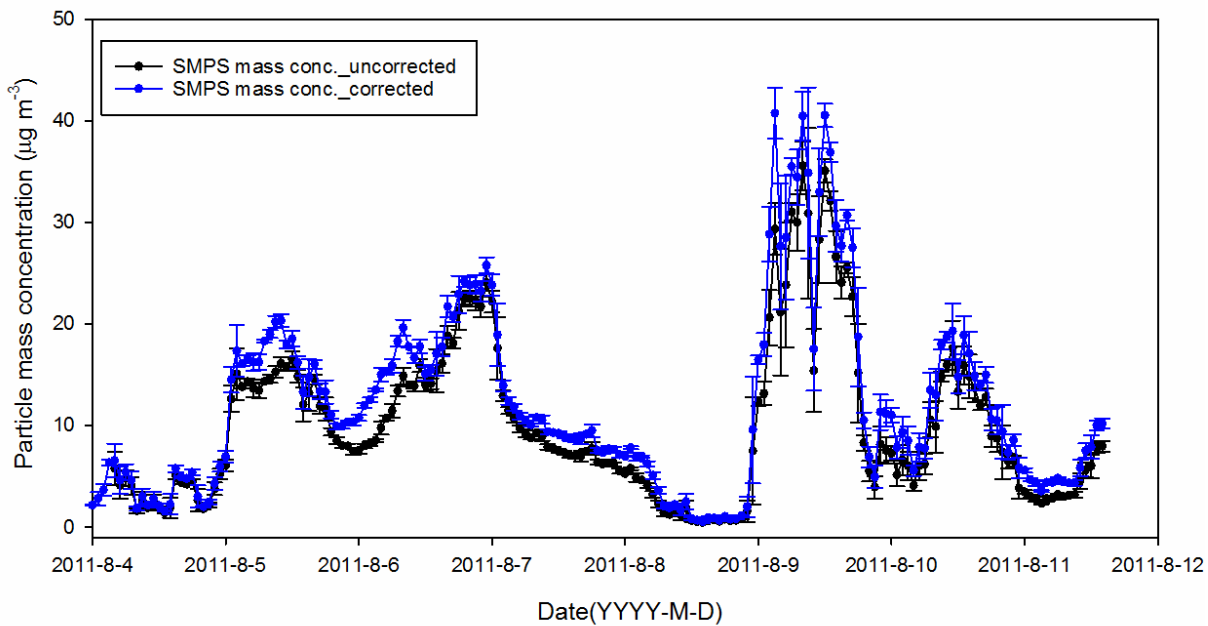
143 We corrected the particle mass concentration measured in PAM reactor with
144 condensation loss by the exiting the reactor and the wall. For AMS measurement, we
145 used a loss of sulfate for sulfate, nitrate, ammonium, and chloride concentration and used

146 a loss of organics for organics concentration. For SMPS measurement, we used a
147 composition dependent loss $(\text{organics}/(\text{organics}+\text{inorganics}) * \text{organics}$
148 $\text{loss} + \text{inorganics}/(\text{organics}+\text{inorganics}) * \text{sulfate loss})$ for the total particle mass
149 concentration. The figure S6 shows the uncorrected and corrected particle mass
150 concentration in PAM reactor. The errors are 2σ confidence. Note that the correction
151 range of the particle mass concentrations were mostly overlapped with the error range.
152

AMS particle mass concentration loss correction



SMPS particle mass concentration loss correction



153
154 [Figure S6. Time series of uncorrected AMS and SMPS particle mass concentration
155 and corrected particle mass concentration with condensable gases loss. The errors are 2σ
156 confidence.]

157
158

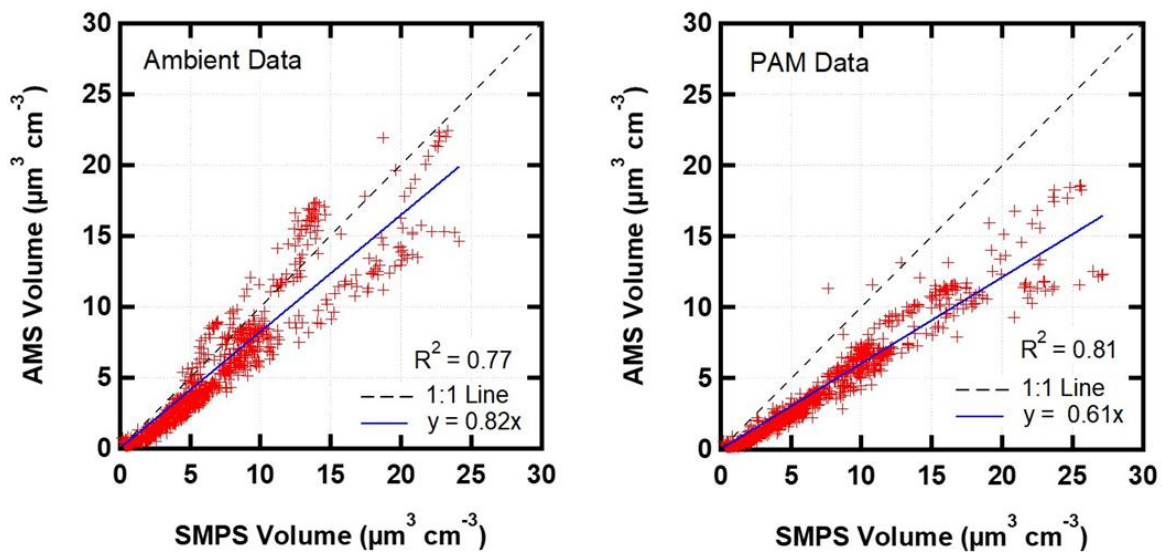
159 S7. A comparison of AMS vs SMPS

160 Aerosol particles volume concentration obtained from AMS and SMPS was compared
161 each other for ambient and PAM aerosol particles. Particle volume concentration from
162 SMPS was directly obtained by the SMPS measurement, and particle volume
163 concentration from AMS was extracted by the measured particle mass concentration
164 divide by composition dependent density.

165
166 Figure 2(c) in the manuscript is a time series of AMS and SMPS particle volume
167 concentration and [Figure S7-1](#) is a scatter plot of AMS and SMPS particle volume
168 concentration. For ambient aerosol particles, the AMS and SMPS particle volume
169 concentrations agree to within measurement uncertainties, but for the PAM aerosol
170 particles, the SMPS volume concentration was greater than AMS volume concentration by
171 a factor of 1.6. While this difference can be explained by the measurement uncertainties
172 of the two instruments, it is also possible that elemental carbon and soil particles are
173 being detected by the SMPS but not by the AMS. In ambient aerosol particles data for
174 the organics-dominated episode, the AMS volume concentration was slightly greater than
175 or similar to that of the SMPS, but in sulfate dominated episode, AMS volume
176 concentration was smaller than that of the SMPS.

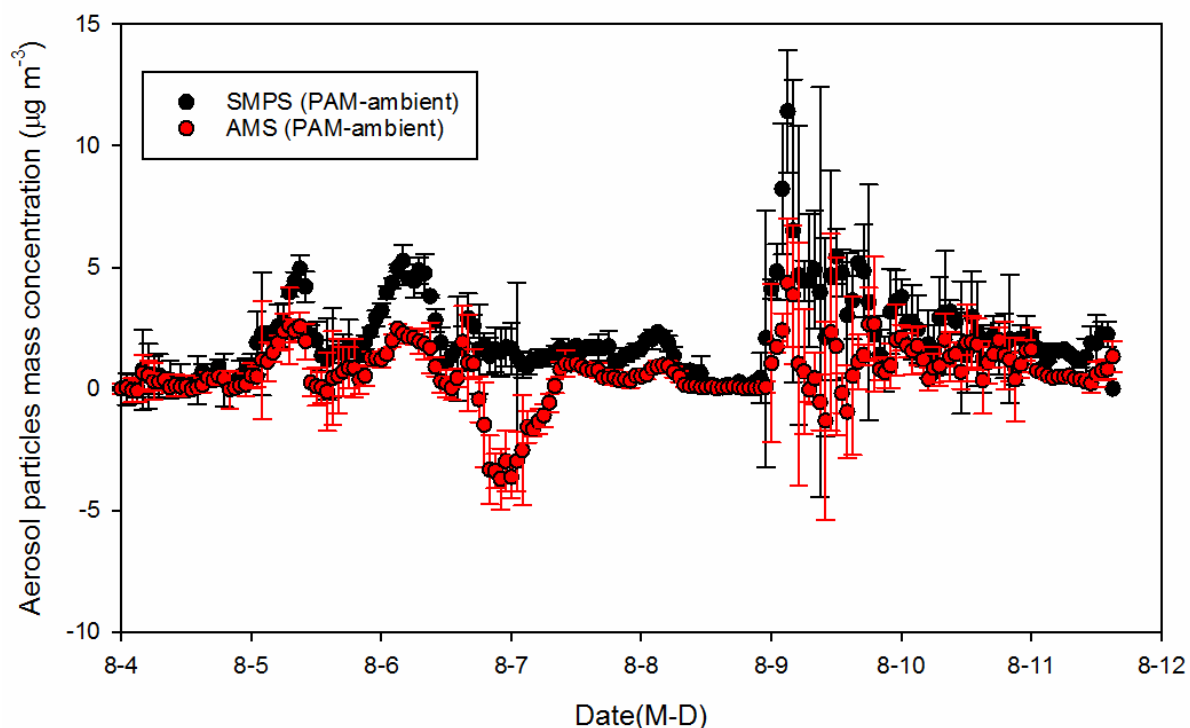
177

178



179
 180 [Figure S7-1. Scatter plots of SMPS aerosol volume concentration and AMS aerosol
 181 volume concentration.]
 182

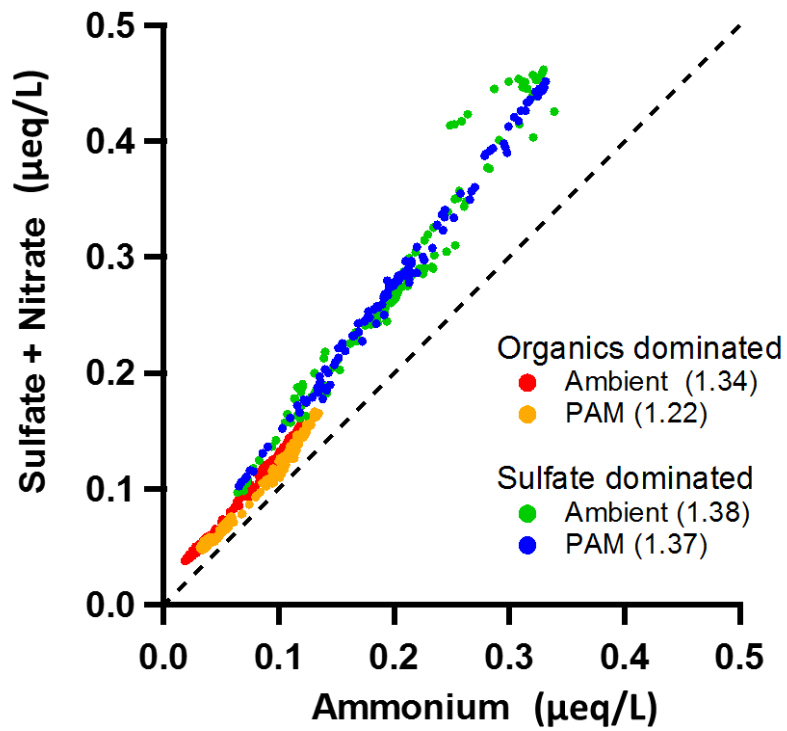
183 The mass concentration changes between the PAM aerosol particles and the ambient
 184 aerosol particles were determined for both the AMS and the SMPS (Figure S7-2). For
 185 most of the data, the SMPS mass concentration difference is equal to or slightly greater
 186 than the AMS mass concentration difference. However, there are also periods during
 187 which the AMS mass concentration difference is much less than the SMPS mass
 188 concentration difference. These discrepancies occur for days when the mass
 189 concentrations are greatest in the organic-dominated period and the sulfate-dominated
 190 period and thus do not depend on the origin of the aerosol particles. The reasons for
 191 these discrepancies are under investigation, but they do not affect our conclusions.



192 [Figure S7-2. The difference in mass concentrations between the PAM aerosol and
 193 ambient aerosol measured by SMPS and AMS. Data are averages for 6 minutes with 2σ
 194 confidence intervals.]
 195

196
 197 S8. Ammonium balance with sulfate and nitrate

198 We plotted the ammonium balance with sulfate and nitrate for ambient and PAM
 199 observation for each episode. The chloride concentration was under $0.4 \mu\text{g m}^{-3}$ which was
 200 less than 1/10 of nitrate concentration, thus we only used sulfate and nitrate. The
 201 inorganic aerosols were overall acidic, and the acidity in PAM aerosol was similar to
 202 ambient aerosol in sulfate dominated episode. It is because of the sulfate enhancement
 203 in sulfate dominated episode while nitrate in PAM reactor was depleted a lot than
 204 ambient nitrate. In organics dominated episode, both of sulfate and ammonium was
 205 enhanced in PAM reactor while nitrate was depleted. Thus, the acidity was rather
 206 decreased in PAM reactor.



207

208 [Figure S8. The normality balance of ammonium with sulfate and nitrate in ambient and

209 PAM aerosol for organics dominated and sulfate dominated episodes. The numbers on

210 the figure legend were the acidity of aerosols obtained from

211 $[\text{sulfate} + \text{nitrate}] (\mu\text{eq/L}) / \text{ammonium} (\mu\text{eq/L})$.

212

213

214

215

216

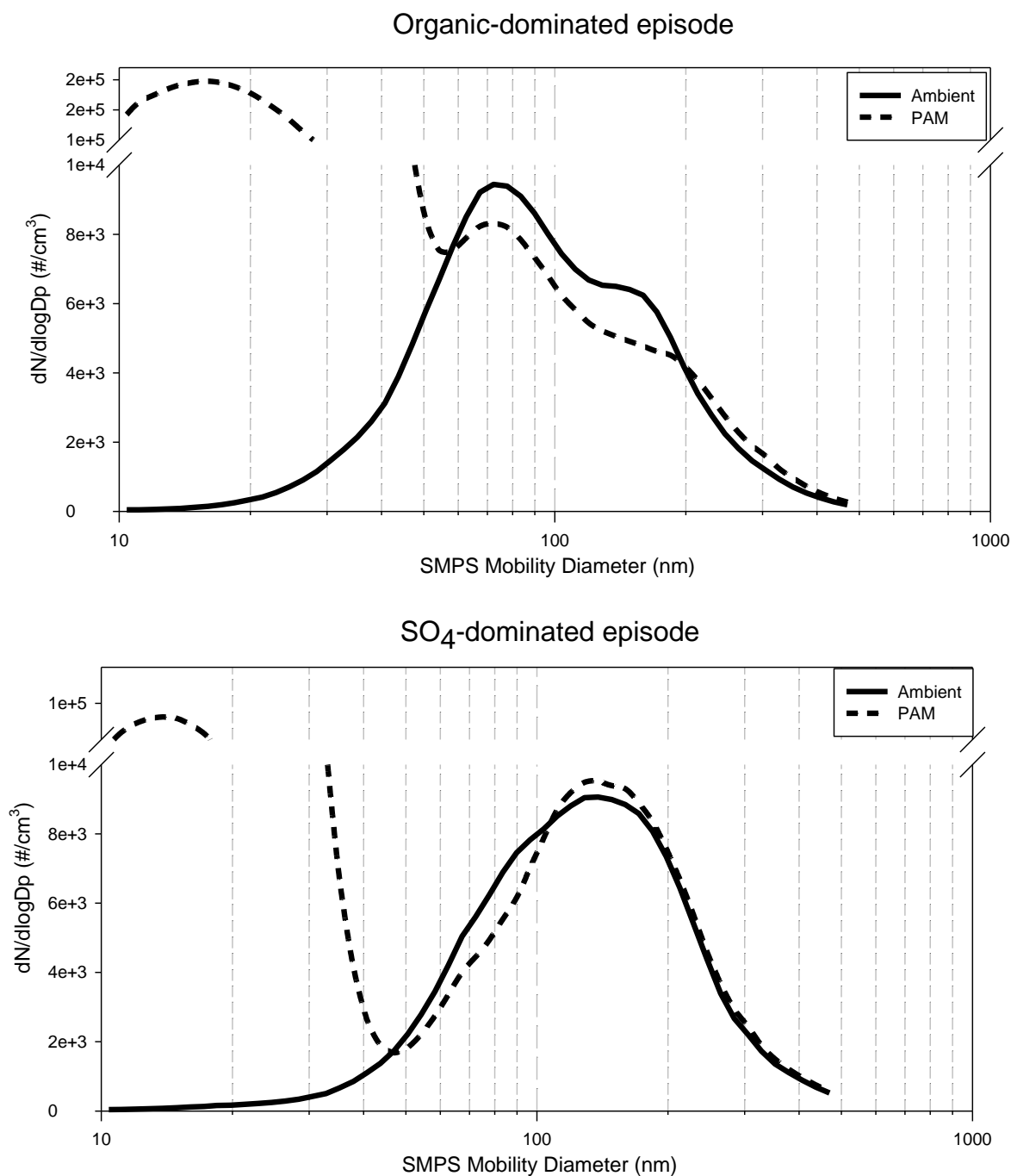
217

218

219

220

221 Figure S9. Ambient and PAM particle size distribution for organic-dominated and sulfate-
222 dominated episode. The $dN/d\log D_p$ ($\# \text{ cm}^{-3}$) of particles smaller than 50 nm in diameter
223 for organic-dominated episode was about an order of magnitude greater than that for
224 sulfate-dominated episode.



225

226 Salimi, F., Crilley, L. R., Stevanovic, S., Ristovski, Z., Mazaheri, M., He, C., Johnson, G., Ayoko,
227 G., and Morawska, L.: Insights into the growth of newly formed particles in a subtropical
228 urban environment, *Atmos. Chem. Phys.*, 15, 13475-13485, <https://doi.org/10.5194/acp->
229 15-13475-2015, 2015.